ON-LINE SPECTRAL MONITORING OF THE VUV FEL BEAM AT DESY

P. Nicolosi, L. Poletto#, M.G. Pelizzo, INFM & Dep. of Information Engineering, Padova (Italy)
J. Feldhaus, U. Jastrow, U. Hahn, E. Ploenjes, K. Tiedtke, HASYLAB-DESY, Hamburg (Germany)

Abstract

A stigmatic spectrometer for the 2.5-40 nm EUV region has been realized. The design consists of a grazing-incidence spherical variable-line-spaced grating with flat-field properties and of a spherical mirror mounted in the Kirkpatrick-Baez configuration that compensates for the astigmatism. The spectrum is acquired on a fluorescent screen optically coupled to an intensified CCD detector, that can be moved along the spectral focal curve to select the spectral region to be acquired. The spectral and spatial resolution of the system have been characterized by using the emission from an hollow-cathode lamp or a laser-produced plasma. At present, the instrument is installed at the VUV-FEL at DESY for the spectral monitoring of the FEL beam in the 20-45 nm region.

INTRODUCTION

The FEL at the TESLA Test Facility (TTF) at DESY achieved first self amplified spontaneous emission (SASE) in the vacuum-ultraviolet in early 2000 [1] and it reached gain up to saturation between 80–120 nm in 2001 [2]. During an on-going upgrade which will be completed at the end of 2004, the VUV-FEL at DESY is being transformed into the worldwide first FEL user facility for vacuum-ultraviolet (VUV) and soft X-ray radiation from 100 to 6 nm wavelength.

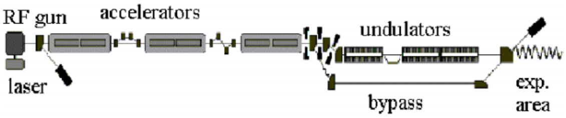

Fig. 1. Layout of the VUV-FEL at DESY

Fig. 1 shows the layout of the linear accelerator. The complete accelerator is currently newly constructed to finally reach energies of up to 1 GeV [3]. A new photoinjector/bunch compression concept is used, and the gun has reached a minimum normalised emittance of 1.5 and 1.7 π mm mrad in the vertical and horizontal plane respectively. In addition, a special collimator system has been designed to protect the undulators, the electron beam focusing along the undulator has been changed, and improved diagnostics have been developed both for the electron and the photon beam. A short accelerator section with third-harmonic cavities to linearize the energy chirp along the electron bunch, which is required for optimum bunch compression, as well as the 6th accelerator module will not be installed into the injector until 2006. Consequently, the wavelength range of the FEL will initially be limited to approximately 20 - 60 nm.

FELs based on self-amplified spontaneous emission produce highly intense, transversely coherent radiation within a single pass of a relativistic electron bunch through a long undulator. The exponential amplification process of a SASE FEL starts from spontaneous emission of the electron beam. Hence, individual radiation pulses differ in intensity, temporal structure, and spectral distribution. Extensive characterization of the FEL beam [4] as well as a first set of experiments on the interaction of such VUV radiation with cluster beams [5] and surfaces [6] was carried out during TTF Phase 1. For commissioning of the VUV-FEL various photon diagnostic units used for beam intensity and profile measurements during the proof-of-principle experiments on TTF1 have been modified and will be installed at the end of the accelerator tunnel, above the electron beam dump. Initial start-up of the FEL is planned in the 30-40 nm spectral region. A grazing incidence grating spectrometer will replace the normal incidence spectrometer used for TTF1 in this area to measure the spectral structure of the FEL pulses on a single shot basis.

An important feature of the SASE FEL pulses is their short duration of 40-200 femtoseconds. An estimate of the pulse duration can be derived from the spectra of the spectrometer already during the commissioning phase, since the spectral width of each peak shown in a single shot-spectrum is related to the radiation pulse length [1].

Tab. 1. Expected parameters of the FEL beam.

Wavelength	100 – 6 nm
Pulse energy	0.1 – 1mJ
Pulse duration (FWHM)	30 – 400 fs
Peak power	0.3 - 2.8 GW
Spectral width (FWHM)	~0.5 %
Spot size at undulator exit (FWHM)	1.4 – 0.14 mm
Angular divergence (FWHM)	170 – 24 μrad
Peak brillance	$1\cdot10^{28}$–$3\cdot10^{30}$ ph/s/mrad^2/mm^2/0.1 %bw

The expected parameters of the VUV-FEL are summarized in Tab. 1 [7]. It is developed into a full user facility with five experimental stations using the FEL beam alternately [3]. Three experimental stations use the direct SASE FEL beam and are equipped with focusing mirrors providing spot sizes of approximately 100 or 10 μm. Two experimental stations for experiments requiring a spectral bandwidth narrower than the natural FEL bandwidth are served by a high resolution plane grating

Contact person: poletto@dei.unipd.it

monochromator, that has a resolution of 80000-10000 while providing a wide tuning range from 10 eV to 1 keV. Alternatively to the monochromator beamlines, the spectral distribution of individual FEL pulses will be determined online by a variable-line-spacing (VLS) grating spectrometer serving the three “SASE beamlines” [8]. One of the plane mirrors in the FEL beam distribution system will be replaced by the VLS grating which reflects most of the radiation in zeroth order to the experiment and disperses only a small fraction in first order for spectral analysis.

The grazing-incidence stigmatic spectrometer that will be used to measure the single-shot spectral structure of the FEL pulses in the 20-46 nm spectral region is presented here. The instrument was designed and realized by the INFM-LUXOR laboratory (Padova, Italy) for absorption spectroscopy on laser-produced plasmas in the 5-45 nm spectral region [9]. The main system requirements are high spatial and spectral resolution and a plane focal curve with the detector used at almost normal incidence, such as in the case of using grazing-incidence spherical variable-line-spaced (SVLS) gratings [10]. The design consists of a SVLS grating with flat-field properties and of a spherical mirror mounted in the Kirkpatrick-Baez configuration that compensates for the astigmatism. The spectrum is acquired on a fluorescent screen coupled to an intensified CCD detector, that can be moved along the spectral focal curve to select the spectral region to be acquired. The spectral and spatial resolution of the system have been characterized by using the emission from an hollow-cathode lamp.

SPECTROMETER DESIGN AND REALIZATION

The design principle of the SVLS grating for flat-field spectrographs is already well established [10] and will be here briefly resumed. The groove density along the grating surface is expressed as

$$\sigma(y) = \sigma_0\left(1 + 2\frac{b_2}{R}y + 3\frac{b_3}{R^2}y^2 + 4\frac{b_4}{R^3}y^3\right) \qquad (1)$$

where σ_0 is the central groove density, R is the grating radius and b_2, b_3, b_4 are the ruling parameters for space variation.

The main aberration to be corrected is the spectral defocusing, which increases linearly with the width of the illuminated area. The spectral focal curve, that is the curve where the spectral defocusing zeroes, is given by

$$\frac{\cos^2\alpha}{r} + \frac{\cos^2\beta}{r'} - \frac{\cos\alpha + \cos\beta}{R} + 2(\sin\alpha + \sin\beta)\frac{b_2}{R} = 0 \qquad (2)$$

where r, r' are respectively the grating entrance and exit arms, and α and β are the incidence and diffraction angles, which are related to the grating equation

$$\sin\alpha - \sin\beta = m\lambda\sigma_0 \, . \qquad (3)$$

To minimize the defocusing on the detector, it is necessary to make the focal curve given by Eq. (2) as close as possible to the detector surface in the spectral range of interest, by acting on the parameters R and b_2. Similarly it can be shown that the parameters b_3 and b_4 can be chosen to minimize coma and spherical aberration.

The main difference between the grazing-incidence SVLS design and the classical grazing-incidence Rowland configuration with uniform-line-spaced gratings is that the focal surface as given by Eq. (2) is almost flat with the detector operated at near normal incidence.

The astigmatism in the plane perpendicular to the plane of spectral dispersion is corrected by a spherical mirror mounted with its tangential plane coincident with the equatorial plane of the grating, i.e. a Kirkpatrick-Baez configuration in which one of the two elements is a grating [11]. The mirror does not provide any focusing in the plane of spectral dispersion, leaving unchanged the grating focal properties given by Eq. (2) that determine the spectral resolution. On the other side, the grating does not provide any spatial focusing, that is in a plane perpendicular to the plane of dispersion, so the spatial performances are determined only by the characteristics of the mirror. The radius of the mirror R_m is determined as

$$R_m = \frac{2}{\cos\theta_m}\left(\frac{1}{p_m} + \frac{1}{q_m}\right)^{-1} \qquad (4)$$

where p_m and q_m are respectively the mirror entrance and exit arms and θ_m is the incidence angle.

It can be shown [9] that such a configuration has also spectral and spatial resolution capability for extended sources (e.g. a laser-produced plasma), due to the Kirkpatrick-Baez configuration that maintains separated the spectral and spatial focal properties on two different optical components. The spectral resolution is constant also for off-axis points, while the spatial resolution decreases with the off-axis distance. In case of a 2 mm source size, the spatial resolution with 5 mrad acceptance angle and a mirror operated at 87° is 25 µm on-axis and 130 µm at the extremes of the field-of-view (i.e. ±1 mm off-axis distance). In other stigmatic designs with spherical or plane VLS gratings, the astigmatism is corrected by an additional mirror mounted on the same plane as the grating [12, 13]: in this case, the spectral and spatial focusing properties are coupled on the mirror and both spectral and spatial resolutions decrease for extended sources far from the optical axis.

The layout of the configuration is shown in Fig. 2. The central groove density of the SVLS grating is 1200 lines/mm; the parameters for groove space variation have been optimized to have an almost flat focal surface in the 10-40 nm spectral region. The calculated focal curve is shown in Fig. 3: it is almost perpendicular to the tangent to the grating on its vertex. Given the low accepted angular aperture of the grazing-incidence system (5 mrad in the spectral plane) and the detector pixel size (20-25 µm), the depth of focus for this system is considered about 5 mm.

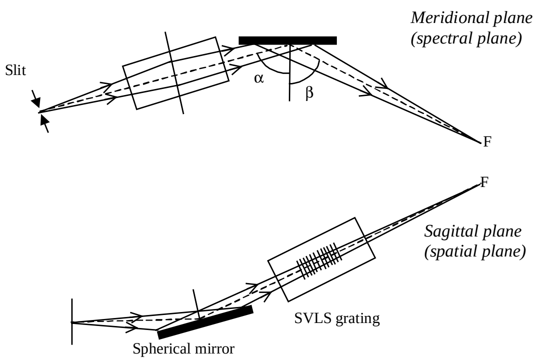

Fig. 2. Layout of the grazing-incidence spectrometer.

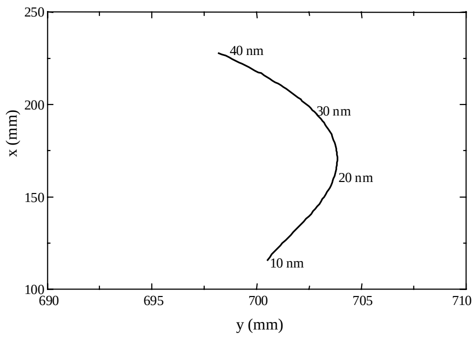

Fig. 3. Spectral focal curve of the SVLS grating. The *x* and *y* axes are defined respectively parallel to the grating normal and parallel to the tangent to the grating on its vertex. The origin of the reference system is the grating vertex.

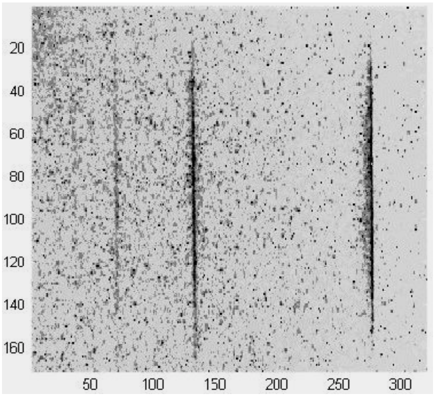

Fig. 4. He spectrum. The wavelength is increasing from left to right. The two most intense lines are HeII 25.6 nm (pixel 130) and 24.3 nm (pixel 275).

The spectrum is acquired on a fluorescent screen optically coupled to an intensified CCD detector. Since the length of the spectrum is larger than the detector size, the latter must be translated along a straight line fitting at the best the focal curve in the region of interest. In order to do this, the detector is mounted on a linear drive and connected to the spectrometer with a system with three laminar bellows. An acquired spectrum is shown in Fig. 4. Additional details of the optical design are presented elsewhere [9].

The parameters of the spectrometer are resumed in Tab. 2.

Tab. 2. Parameters of the spectrometer.

Accepted aperture	5 mrad (spectral plane) 10 mrad (spatial plane)
Spherical mirror	
Entrance/exit arms	400 mm / 1000 mm
Incidence angle	87.5°
Coating	Gold
SVLS gratings	
Central groove density	1200 gr/mm
Spectral range	5-50 nm
Entrance/exit arms	650 mm / 750 mm
Incidence angle	87°
Coating	Platinum
Detector	
Phosphor screen diameter	25 mm
Objectives	50 mm f/1.0 105 mm f/1.8
Intensified CCD camera	MCP and cooled CCD
Detector format	1280 pixel $\times$ 1024 pixel

INSTRUMENT PERFORMANCE

The spectrometer was aligned and calibrated in the 24-46 nm spectral region using as source an hollow-cathode lamp. The measured performance are very close to the theoretical predictions: the spectral lines have FWHM of about two pixels. Being the optics aligned at the best, the detector was positioned on the straight line fitting at the best the spectral focal curve. The spectral region of operation is selected by moving the detector along this straight line. An absolute encoder gives the relative translation of the detector with respect to a reference point.

The system calibration is divided in two steps: 1) the measurement of the detector scale factor and 2) the wavelength calibration.

The scale factor (μm/pixel) expresses the size of the phosphor screen imaged in one CCD pixel: it has been measured as 8.0 μm/pixel.

The wavelength calibration is performed by measuring the position of the focal plane with respect to the grating vertex. The parameters that allow to identify the detector plane (i.e. the straight line where the detector is moved) are calculated by acquiring some known spectra from the hollow-cathode source together with the encoder measurements on the detector position, and then applying a fitting procedure. The residual calibration errors are less than 0.03 nm and are mainly due to the intrinsical precision of the encoder.

The actual spectral dispersion is shown in Fig. 5 assuming 32 μm pixel size (i.e. a binning factor of 4 on the CCD). The resolution, calculated as the ratio $\lambda/\Delta\lambda_{2px}$ with $\Delta\lambda_{2px}$ evaluated within two pixels, is 1500@30 nm and 1900@45nm, definitely higher than the expected FWHM of the FEL emission.

Some calibrated spectra are finally shown in Fig. 6.

At present, the instrument is installed at the VUV-FEL at DESY for the spectral monitoring of the FEL beam in the 20-45 nm region.

REFERENCES

[1] J. Andruszkow et al, Phys. Rev. Lett. 85 (2000), 3825
[2] V. Ayvazyan et al, Phys. Rev. Lett. 88 (2002), 104802
[3] http://www-hasylab.desy.de
[4] R. Ischebeck et al, Nucl. Instr. and Meth. A 507 (2003), 175
[5] H. Wabnitz et al, Nature 420 (2002), 482
[6] A. Andrejczuk et al, HASYLAB An. Rep. 1 (2001), 117
[7] K. Tiedtke et al, to be published in AIP Conf. Proc. 2004 (SRI 2003, San Francisco, CA, U.S.A.)
[8] R. Reininger et al, to be published in AIP Conf. Proc. 2004 (SRI 2003, San Francisco, CA, U.S.A.)
[9] L. Poletto et al, Appl. Opt. 41 (2002), 172
[10] T. Harada and T. Kita, Appl. Opt. 19 (1980), 3987
[11] L. Poletto and G. Tondello, Appl. Opt. 39 (2000), 4000
[12] P. Fan et al, Appl. Opt. 31 (1992), 6720
[13] M. Hettrick and S. Bowyer, Appl. Opt. 22 (1983), 3921

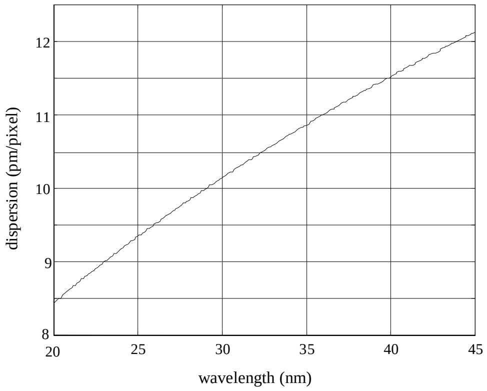

Fig. 5. Actual spectral dispersion. The pixel size is assumed 32 μm.

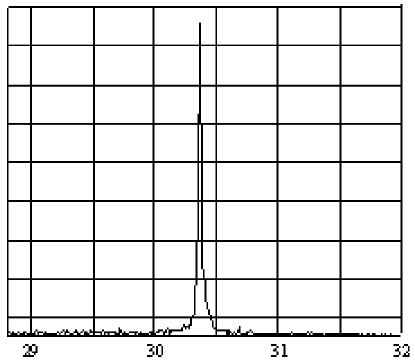

a)

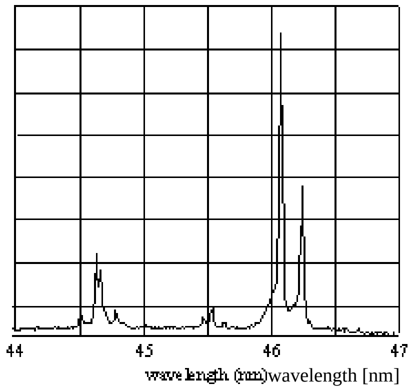

b)

Fig. 6. Spectra acquired with the hollow-cathode lamp. The plots are horizontal cross-sections across the CCD image. a) He spectrum (HeII 30.4 nm line); b) Ne spectrum (NeII 44.62, 44.66, 46.07 and 46.24 nm lines).